INTEGRATION OF HIGH RESOLUTION MULTISPECTRAL IMAGERY WITH LIDAR AND IFSAR DATA FOR URBAN ANALYSIS APPLICATIONS

P. Gamba[1],
[1]Department of Electronics
University of Pavia
Italy
gamba@ele.unipv.it

B. Houshmand[2]
[2] Jet Propulsion Laboratory
California Institute of Technology
CA, USA
bh@athena.jpl.nasa.gov

KEY WORDS: Urban analysis, data fusion, Interferometric SAR.

ABSTRACT

This paper presents the integration of 50 cm 4 band (R, G, B, and infrared) imagery with 80 cm LIDAR, and 2.5 meter posting IFSAR surface elevation models for urban scene analysis. The goal is to characterize urban scenes in terms of buildings, trees, roads, other geometrical structures, open areas, and various natural land covers. This type of information is useful for applications such as urban monitoring, change detection, and urban scene visualization. In this paper we present some of our recent findings for automated extraction of buildings, and integration of multiple sensors for landcover classification and feature extraction. In addition, we present a comparative analysis of the digital surface model provided by Laser altimeter, and Interferometric Synthetic Aperture Radar (IFSAR). The algorithms presented in this paper are applied to an urban area composed of isolated and dense built areas, trees, and natural topography.

1 INTRODUCTION

Geographical information of urban areas is useful for a number of applications such as mission planning, monitoring of urban change and growth, and environmental impact studies. Remote sensing of urban areas provide an efficient methodology for populating databases for geographical information systems (GIS). These remote sensing methodologies include stereo optical photogrametry, multispectral and hyperspectral imaging, Light detection and Ranging (LIDAR), Synthetic Aperture Radar (SAR), and Interferometric Synthetic Aperture Radar (IFSAR). The information provided by these measurement technologies can be divided into two categories: Land Cover, and three dimensional geometry. Multispectral and hyperspectral imaging and SAR measurements capture the land cover properties of a scene. Stereo Optical, LIDAR and IFSAR measurements provide the 3 dimensional information for a scene. The reflectance associated with these measurements is used to provide land cover information associated with the three dimensional geometry. The amount of efforts in terms of data acquisition and post processing varies significantly among these remote sensing methodologies. IFSAR systems provide fast data acquisition with near all weather, all time imaging capability. In this paper, we investigate the use of IFSAR and LIDAR sensors to create three dimensional information of an urban area. We also use a multispectral data to provide land cover information for the same scene. The use of land cover information is particularly useful for the interpretation of IFSAR data which contains artifacts due to radar multi-scattering effects.
Next section is devoted to the description of the segmentation procedure of the DEM data. Section 3 outlines the procedure for integration of IFSAR and multi-spectral data for generating an improved DEM model which contain the bald earth topography in addition to large geometrical structures. Sample results are shown in section 4 using radar (2.5 meter posting), multi-spectral (50 cm posting), and LIDAR (80 cm posting) data. Concluding remarks are in section 5.

2 A PLANE-FITTING REGULARIZATION ALGORITHM

In machine vision, it is usual to deal with 3D (also called *range*) images, and the major problem is to segment them to obtain surfaces that could be matched against some kind of surface model. The surface parameters may be computed by fitting the model and the data. This kind of approach can suitably describe the largest part of the approaches that have been and are presently developed in the field of LIDAR data analysis, with the exception of all the algorithms devoted to discriminate between buildings and vegetation.

In this work we want to introduce a recently developed algorithm for surface extraction and analysis, whose primary goal was to enhance the 3D geometry retrievable from interferometric SAR measurements. Indeed, it is well-known that this kind of data are affected by bounce effects of the radar pulse that cause false objects to appear. These phenomena, that are called layover and shadowing effects, produce a (possibly large) distortion of the 3D structure of the buildings in a urban, crowded environment. Therefore, a simple segmentation algorithm, with surface model fitting does not provide results of any interest if we start from these data. The algorithm has been introduced in Gamba and Houshmand, 1999 and will be soon available a longer and more precise paper (Gamba et al.,). In the following we give a quick outline of the procedure, and then we will see that, although not primarily suited for the task, it could be used for LIDAR data analysis with satisfying (but not excellent) results.

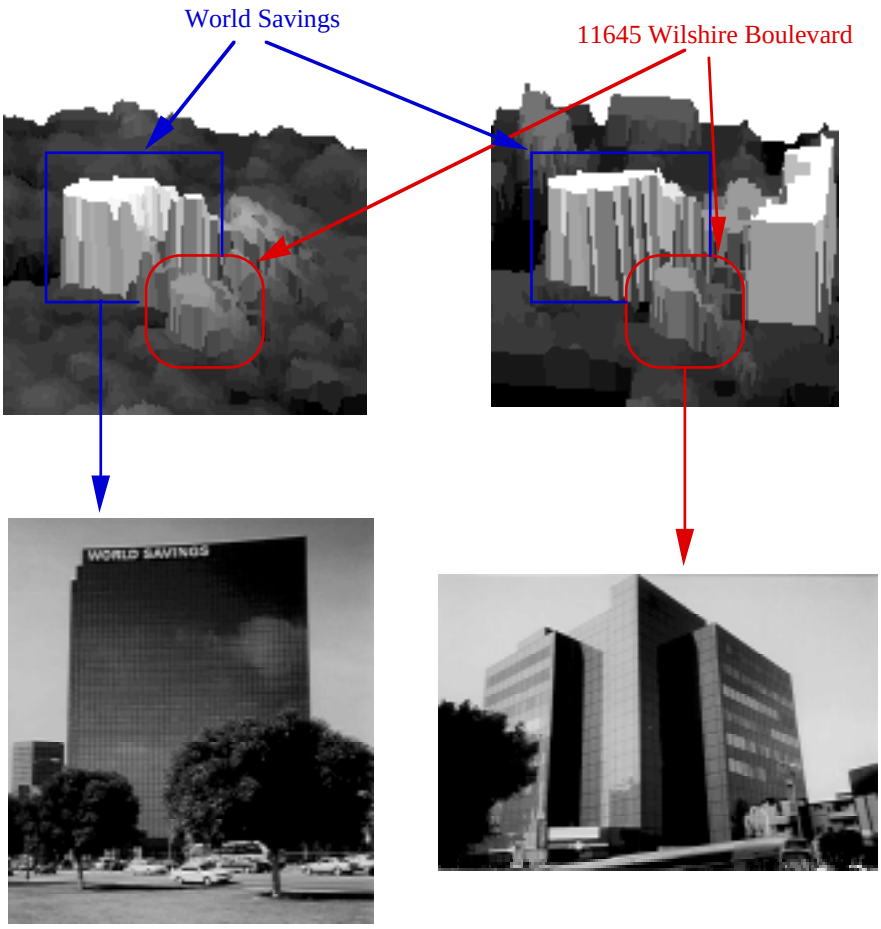

Figure 1: The original (*top left*) and extracted shapes (*top right*) of two buildings in S. Monica, Los Angeles. The starting data was a 2.5 m posting TOPSAR DTM.

Note that, since the algorithm was devised for use with data highly affected by noise, it was suited so to exploit both the spatial and vertical resolutions of the original data, while maintaining at the same time a high robustness to noise. In particular, the criteria applied to segment the raw data are geometric ones, involving the principle of plane-fitting (i.e. to find the plane which better approximates a given surface). The idea is justified by the rough consideration that a building extraction approach should be able to detect first of all the roofs and walls of a given, observed structure. Such an idea could not be realized by means of a simple iterative region growing approach. Instead, the algorithm is a refined and adapted version of the range image segmentation procedure first presented in Jiang and Burke, 1994.

The algorithm starts from primitives of segmentation that are the lines of the image, in order to save cpu time as much as possible, and it works by means of five processing steps.

1. First of all, the procedure works on each image line by trying to group the pixels into consistent segments. The grouping is ruled by two parameters: the first one allows to join points with a step between them up to its value, while the second one determines the minimum length of each segment. By this way we may rule the regularization process, even if the choice should be careful. Indeed, by enlarging the first threshold we allow to recover from possible outcomes in the measurements, but we run the risk to give too much weight to isolated points. The second threshold, instead, is defined by the data resolution and the precision we want to have for edge detection. Even in this case the compromise is between smaller segments (smaller final regions, less surface regularization) and poorer edge (region boundaries) detection. We found that, for radar measurements it is possible to suitably choose these parameters, while for LIDAR data the problem is harder. Anyway, it is a good practice to set this length as small as possible with respect to the physical characteristics of the buildings to be extracted and the resolution of the image.

2. The second step consists in finding the *seeds* for the planar surfaces that we want to use to characterize the original image. Differently from the previous version of the algorithm presented in Gamba and Houshmand, 1999, each seed is found by looking only for two adjacent segments belonging to two successive scan lines and with the most similar direction and z-axis intercept. So, similarity search is based on the following measure:

$$s_{ij} = \frac{1}{2}\left(\frac{m_i m_j + 1}{\sqrt{m_i^2 + 1}} + \frac{n_i n_j + 1}{\sqrt{n_i^2 + 1}} \right) \qquad (1)$$

where $z = m_i x + n_i$ is the generic segment equation. One of the reasons for this simple seed choice is just its simplicity; however, the main reason is that, dealing with complex buildings, the number of three-segment seeds that we may find is definitely lower than the one of two-segment seeds. Therefore, the successive region growing procedure may suffer from this problem and aggregate only a small number of other segments to the original seeds.

3. The third step is devoted to the enlargement of the seed just found. The task is accomplished by examining all the segments that *touch* in some way any seed, and whose parameters may be considered sufficiently similar to the seed ones. Again, the similarity is defined by means of (1). The research is made for all the isolated segments, and repeated until all of them have been added to a planar surface, or no further aggregation is possible. It is clear that a lower similarity threshold provides a larger regularization of the detected surfaces, but it is also possible that erroneously positioned segments, detected in the first step, produce a negative effect on the final result. To exclude the problem, it is necessary to require a high similarity before aggregation and this in turn produces a large number of segments that, at the end of this step, give no contribution to surface detection.

4. To recover from what could be considered as an inaccuracy of the procedure, a further merging step takes into account separately all pixels left. In other words, we now neglect the segment analysis of the first step for all those pixels that have not been aggregated into a plane, and we try to merge them one at a time with the nearest plane. Even in this case the process is repeated after each computation of the plane parameters. By this way, we take into account the newly added points in the successive iteration.

5. Finally, the recovered planes may be connected into more complex regions if they are adjacent and their characteristics are similar, i. e. again:

$$s = \frac{1}{3}\left(\frac{aa' + 1}{\sqrt{a^2 + 1}} + \frac{bb' + 1}{\sqrt{b^2 + 1}} + \frac{cc' + 1}{\sqrt{c^2 + 1}} \right) \qquad (2)$$

is close to one, *a, b, c* being the three parameters identifying a plane.

Even after all these joining steps, it is still possible that a few pixels have not been considered in the final results. A this point, however, we do not consider it as an inaccuracy of the

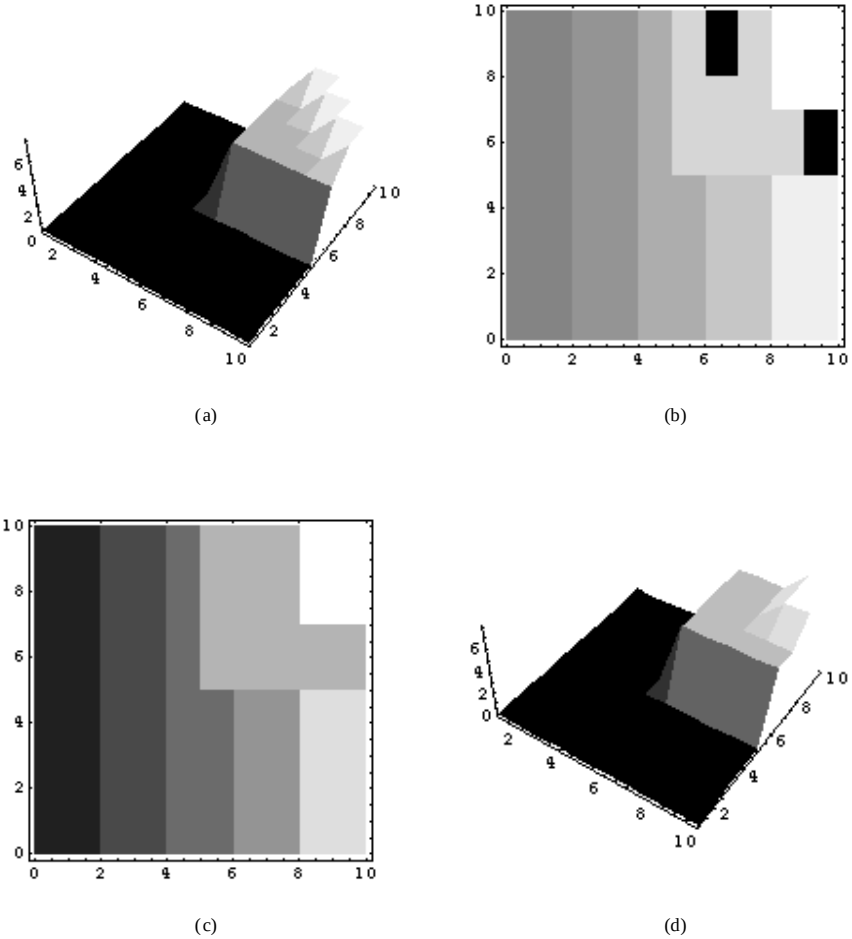

(a) (b) (c) (d)

Figure 0. Some of the processing steps of the building extraction procedure: (a) the original data; (b) the region obtained by segment aggregation; (c) the region obtained by point and plane aggregation; (d) the final reconstructed

algorithm. Indeed, points affected by large noise, or regions where no actually planar surface is observable should not be aggregated, if we want to produce a meaningful segmentation of the original data.

An example of the regularization of radar data achieved by means of this algorithm may be found in figure 1, where the original and analyzed 3D profile of a small portion of Wilshire Boulevard, S. Monica, CA, is shown. In the figure we may recognize that the two major buildings, namely World Savings and 11645 Wilshire Boulevard, are more clearly devised after the detection procedure. Moreover, even if it not provided in the image, both of them were available as independent structures, as set of planar surfaces.

Figure 2, instead, provides a way to understand how the plane growing procedure acts through steps 3, 4, and 5 of the algorithm. Indeed, we may observe the original data (in this case, a very simple test image), the boundaries of the planar regions initially detected, the final regions obtained after segment, point and plane aggregation, and the final result. Here black pixels represent areas that we were not able to characterize.

3 DATA FUSION OVER URBAN ENVIRONMENTS

Urban three dimensional (3D) geometry and land cover are among the information required for urban analysis. Current LIDAR systems are providing urban digital surface model with cm level accuracy. LIDAR high resolution data acquisition, however, is more time consuming in comparison with IFSAR. IFSAR systems provide a coregistered planimetric digital elevation model and radar intensity image. The IFSAR generated digital elevation model accuracy is typically in the meter level range for natural topography. For urban areas, the surface model accuracy degrades due to shadowing, and layover effects. The surface model derived from either sensor requires additional processing to extract the bald earth topography, and geometrical features such as buildings. The synthetic aperture radar intensity image provides a high resolution description of the urban land cover. The SAR image is sensitive to landcover properties such as the texture, material, and geometrical structures. It is also dependent on the radar operating frequency, polarization, and radar view angle. In addition, the radar intensity image is sensitive to the orientation of the imaged geometry with respect to the radar platform. Figure 3 shows the SAR intensity image of the study area. This area is near the Gold Gate bridge in San Francisco, California. Image pixel size is 2.5 meters, and the radar operating frequency is X-band (3 cm wavelength). The image is composed of dense urban area, areas covered by large trees, open, as well as isolated building structures of various dimensions. The dark region on the upper left corner of the image corresponds to the water. We use the land cover information provided by the high resolution multispectral sensor to assist with interpretation of the SAR image at meter level scale.

Integration of multispectral data with the IFSAR generated DEM is carried out in two steps. First the multispectral data is segmented into physically descriptive classes, such as vegetation, building footprints, bodies of water, and features such as road network. This information is then used to located these areas in the IFSAR digital elevation model.

The integration of the land cover data is particularly useful for interpretation of the topography generated by IFSAR data. Land cover classification provided by the multispectral sensor allows the delineation of the areas where the topography interpretation is more straight forward, such as open regions. We use this information to create a background (bald earth) topography from the IFSAR data. The information regarding the building structures are added to the bald earth topography using the building footprint information which is

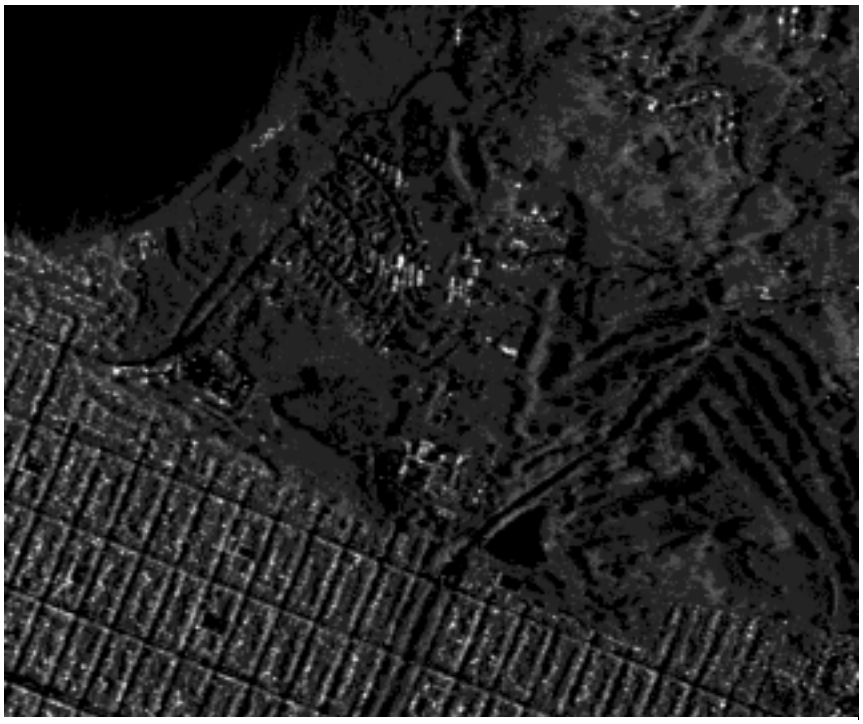

Figure 3: X-band SAR data over the Presidio area, S. Francisco, CA.

Figure 4: Integration of multispectral with SAR data over the same area as in fig.3.

derived from the multi-spectral data, and the height information derived from the IFSAR data. The vegetation height is also included in the final digital surface model as the difference between the background topography and the IFSAR generated elevation model. The resulting digital elevation model includes the background topography, location and average height of building structures which are observable in the multispectral image, and the natural topography such as trees and open fields.

We note that the accuracy of the of the resulting topography is dependent on the generated bald earth topography as well as the accuracy of the height measurements by the IFSAR system. The height reported for regions covered by trees correspond to the top of tree canopies for the X-band frequency range. For lower operating frequencies, the reported height might correspond to elevation level below the tree canopies. The height reported for building tops are typically accurate since the radar backscattered signal is strong from such geometrical structures. The main error source in height values in the urban areas is due to layover effects where a large structures affect the height measurement of the neighboring areas, and the

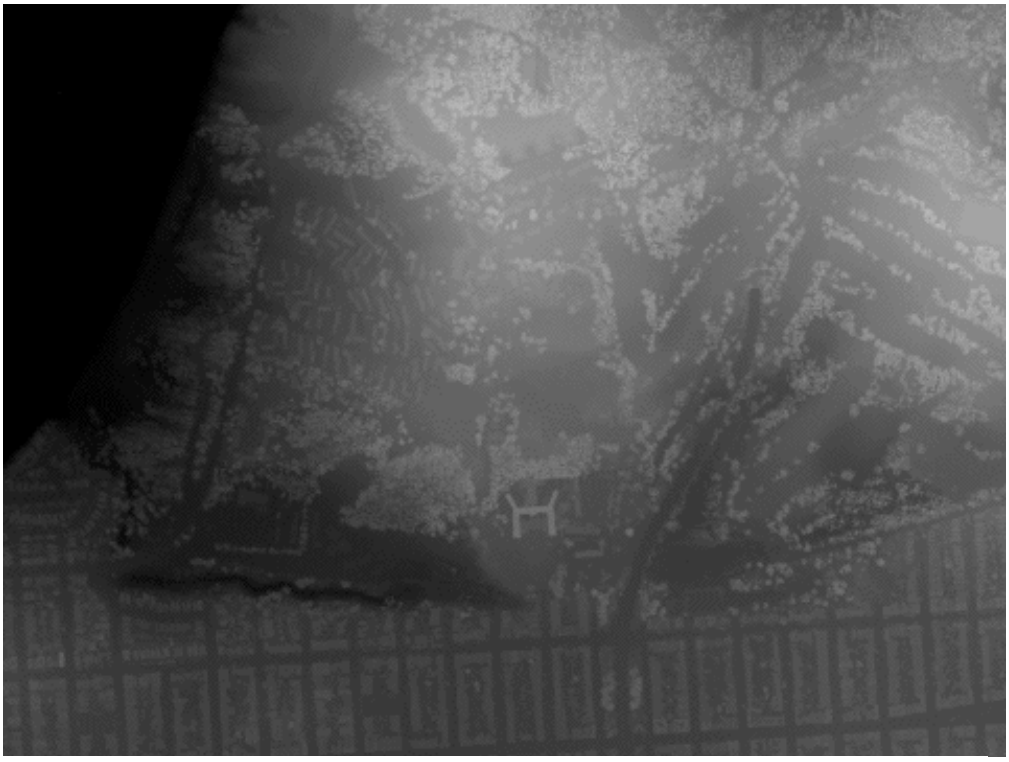

Figure 5: 80 cm posting LIDAR data over the Presidio area.

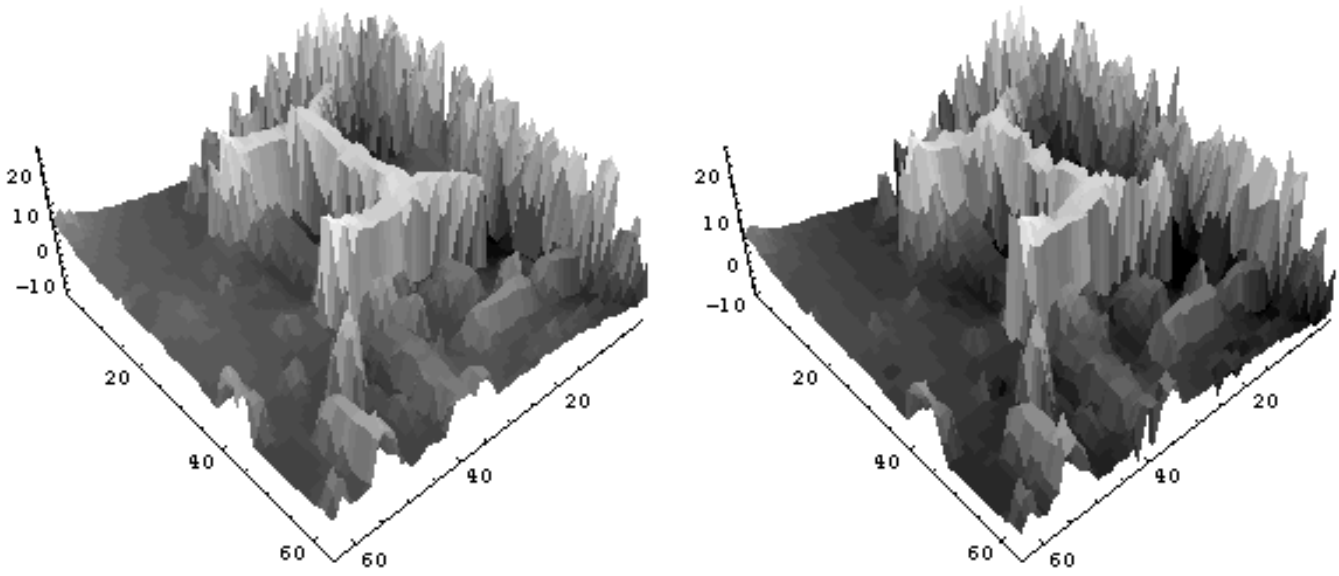

Figure 6: the original LIDAR of a large structure in the Presidio area (*left*) and its reconstructed planar patch approximation (*right*)

shadowing effect, where some structures are not illuminated by the radar signal.

4 EXPERIMENTAL RESULTS

A portion of the Presidio area in San Francisco, California is used for this study. This area contains natural topography such as hills, open areas, tree covered areas in addition to buildings of small to moderate footprint and heights. The IFSAR data is acquired from an airborne X-band, 80 MHz IFSAR system. The IFSAR digital elevation model, and the associated radar intensity image are reported on a 2.5 meter grid. Figure 3 shows the radar image of the region. 50 cm resolution aerial image of a portion of this region is overlaid on the SAR image to assist with segmentation of the corresponding IFSAR DEM. Figure 4 shows the integrated SAR and multi-spectral image. The location of tree covered regions, building, and open areas are clearly observable in this image.

Figure 5 is a LIDAR height image of the same region. The LIDAR data is reported on a 80 cm grid. As expected for high resolution LIDAR data, the building geometries are observable for large and small structures. The regions covered by trees are denoted by a texture which is distinct from the neighboring areas.

Fig. 6 shows an example of the building extraction algorithm, applied to a large structure (an hospital) in the same area. The reconstructed 3D shape, obtained by starting from LIDAR data, is now made by a very small number of planar patches. Moreover, many of these patches are similarly orientated, as we expect in a man-made object. If near patches have higher orientation variance, probably it is because they belong to tree or to natural surfaces. This is a property that we would like to investigate in the future.

The purpose of integrating the IFSAR image with the multi-spectral data is to produce a DEM which contains the main features of the LIDAR DEM data within the height accuracy corresponding to the radar system noise level. The DEM features which we focus on include the large building structures, height variations over tree covered regions, and the bald earth topography. The accuracy of height values for small structures is low due to IFSAR system level noise level.

Figure 7 shows an example of the generated DEM using the IFSAR generated topography and the multi-spectral image. The multi-spectral data is used to delineate the open areas. A bald earth topography is generated by a low pass interpolation of the IFSAR DEM in these regions. The building heights are determined using the height distribution in the footprint of each building detected from the multi-spectral data. We note that this procedure results in flat top buildings, and the corresponding height values are interpreted as the average heights for the building structures. For the regions covered by vegetation, the vegetation height is the difference between the background topography and the IFSAR DEM. A comparison of the resulting DEM with the LIDAR data indicates that the height of large building structures are determined within ±2 meter level accuracy.

These results indicate that while a pixel level DEM accuracy of this procedure is not as accurate as high resolution LIDAR data, the general topography characteristics, and the dimensions of dominate structures are represented well.

5 DISCUSSIONS AND CONCLUSIONS

High resolution Interferometric SAR can provide useful information for urban environment in terms of the three dimensional geometry. The data quality is improved by using landcover information derived from multi-, or hyperspectral data. This type of data integration provides a methodology to remove the radar artifacts which are associated with urban

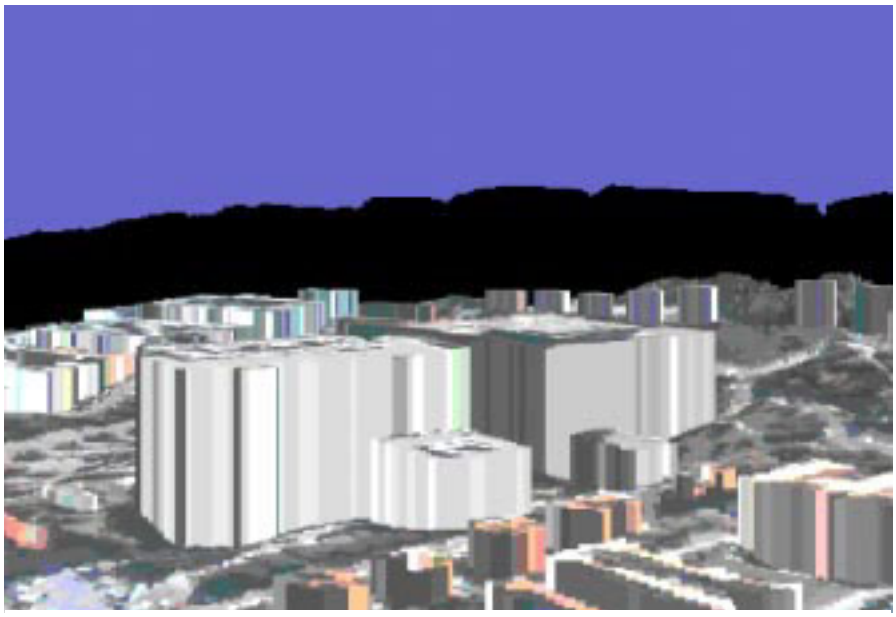

Figure 7: an example of DEM generated by fusion of multispectral and IFSAR data.

environment such as layover effects. Our study shows that LIDAR provides a more accurate representation of urban three dimensional geometry. The IFSAR data can be used to extract isolated features such as a tall building, and the bald earth topography.

REFERENCES

Burkhart, G.R, Bergen, Z., Carande, R., Hensley, W., Bickel, D., Fellerhoff, J.R., 1996. Elevation correction and building extraction from Interferometric SAR imagery. In: IGARSS'96}, Vol. I, pp. 659-661, Lincoln, Nebraska.

Brunn, A. and Weidner, U., 1998. Hierarchical Bayesian nets for building extraction using dense digital surface models. ISPRS J. Photogramm. Remote Sensing, Vol. 53, No. 5, pp. 296-307.

Gamba, P., and Houshmand, B., 1999. Three-dimensional urban characterization by means of IFSAR measurements. In: IGARSS'99, Vol. V, pp. 2401-2403, Hamburg, Germany.

Gruen, A., 1998. TOBAGO -- a semi-automated approach for the generation of 3-D building models. ISPRS J. Photogramm. Remote Sensing, Vol. 53, No. 2, pp. 108-118.

Gruen, A. and Wang, X., 1998. CC-modeler: a topology generator for 3-D city models. ISPRS J. Photogramm. Remote Sensing, Vol. 53, No. 5, pp. 286-295.

Jiang, X. and Bunke, H, 1994. Fast segmentation of range images into planar regions by scan line grouping. Machine Vision and Applications, No. 7, pp. 115-122.

Haala, N. and Brenner, C., 1999. Extraction of buildings and trees in urban environments. ISPRS J. Photogramm. Remote Sensing, Vol. 54, No. 2-3, pp. 130-137

Henderson, F.M. and Xia, Z.G., 1997. SAR applications in human settlement detection, population estimation and urban land use pattern analysis: a status report. IEEE Trans. on Geoscience and Remote Sensing, Vol. 35, No. 1, pp. 79-85.

Maas, H.-G. and Vosselman, G. , 1999. Two algorithms for extracting building models from raw laser altimetry data. ISPRS J. Photogramm. Remote Sensing, Vol. 54, No. 2-3, pp. 153-163.

Weidner, U. and Forstner, W., 1995. Towards automatic building extraction from high resolution digital elevation models. ISPRS J. Photogramm. Remote Sensing, Vol. 50, No. 4, pp. 38-49.